

Propulsion Control of a Large Civil Aircraft using On-line Control Allocation

Halim Alwi and Christopher Edwards

Abstract— This paper explores the possibility of controlling an aircraft using only engine thrust in the event of total control surface failure (due to the loss of hydraulics) using an on-line sliding mode control allocation scheme. Here, both lateral and longitudinal fault tolerant control (FTC) of a non-linear model of a civil aircraft is presented. The simulations have been undertaken using software called FTLAB747. The effectiveness level of the actuators is used by the control allocation scheme to redistribute the control signals to modulate engine thrust when a total hydraulic failure occurs. The simulation results from the non-linear model give good performance and show it is still possible to bring the aircraft to a near landing position without restructuring the controller.

I. INTRODUCTION

Most of the aircraft fault tolerant control (FTC) literature deals with actuator redundancy that can be used to regain control, stability and even performance, in the presence of faults and failures. Most of the faults or failures considered are associated with particular control surfaces and therefore usually other ‘redundant’ control surfaces can be used to overcome these difficulties (e.g. in a civil aircraft, the horizontal stabilizer can be used if elevator faults or failures occur). However in some cases, overall control of all surface actuators can be lost – for example due to failures in the hydraulic systems. Even though the likelihood of a total loss of hydraulics is very small due to hardware redundancy, (triple redundancy is present in most large transport aircraft [5]), there is still a possibility of it occurring – as reported in some incidents during the last 20 years (see [7] for specific examples). These incidents motivated NASA [7], [9], [8], [6] and some researchers [21], [15] to study the use of engine only flight control. Researchers in NASA simulated and flight tested the propulsion controlled aircraft (PCA) concept to show that an aircraft can be controlled using only the engines.

In terms of FTC, sliding mode control (SMC) combined with control allocation (CA), has great potential for the development of simple, robust fault tolerant flight controllers [1]. Shin *et al.*[22], Wells & Hess [29] and Shtessel *et al.*[23] have all proposed sliding mode FTC for aircraft. However, no-one (as far as the authors are aware) has worked on sliding mode controllers for the situation of total hydraulic failure. This paper describes a design and analyzes the associated performance of a sliding mode FTC scheme using CA for the non-linear aircraft model FTLAB747 [19], [24]. Much of the earlier literature using this software has considered only longitudinal control (apart from [18],

[15]). In the work in [15], a propulsion controlled aircraft is considered under the assumption that the engines have thrust vectoring capability, which, with current technology, is only available on advanced modern military aircraft like the Gripen. Recent results using FTLAB747 from the GARTEUR AG16 programme ([2], [26], [17], [13], [10]) consider several types of actuator failures (e.g. an elevator jam and rudder runaway) and the ELAL flight 1862 incident [24]. However, total hydraulic failure was not considered. This paper will demonstrate the capabilities of the theoretical ideas from [1] when handling total loss of hydraulics on a realistic and high fidelity 77 state non-linear model of a civil aircraft. The idea is to design longitudinal and lateral sliding mode controllers with online control allocation that can be used for both nominal and failure conditions without reconfiguring or restructuring the controller. In the event of a total hydraulic failure, the control signals are redistributed to the remaining functioning ‘actuators’ (i.e. the engines) to regain stability, and some level of performance to allow a safe landing.

II. CONTROLLER DESIGN

This paper considers a system of the form

$$\dot{x}(t) = Ax(t) + Bu(t) - BK(t)u(t) \quad (1)$$

where $A \in \mathbb{R}^{n \times n}$ and $B \in \mathbb{R}^{n \times m}$. The effectiveness gain $K(t) = \text{diag}(k_1(t), \dots, k_m(t))$ where the $k_i(t)$ are scalars satisfying $0 \leq k_i(t) \leq 1$. These scalars model a decrease in effectiveness of a particular actuator. If $k_i(t) = 0$, the i th actuator is working perfectly whereas if $k_i(t) > 0$, a fault is present, and if $k_i(t) = 1$ the actuator has failed completely. In this paper, information about $K(t)$ will be incorporated into the allocation algorithm through a weighting matrix W . The information necessary to compute K (and hence W) can be supplied by a fault reconstruction scheme as described in [27] for example, or by using a measurement of the actual actuator deflection which is available in many systems e.g. passenger aircraft [5]. The idea is that if an actuator fault occurs, the weighting W is changed on-line and the control input $u(t)$ is reallocated to minimize the use of the faulty control surfaces.

In much of the control allocation literature it is assumed that $\text{rank}(B) = l < m$. The input distribution matrix B is then factorized as

$$B = B_\nu N \quad (2)$$

where $B_\nu \in \mathbb{R}^{n \times l}$, $N \in \mathbb{R}^{l \times m}$ and both have $\text{rank } l < m$ [16]. A ‘virtual control input’ is then defined as

$$\nu(t) := Nu(t)$$

Halim Alwi and Chris Edwards are with the Control and Instrumentation Research Group, Department of Engineering, University of Leicester, University Road, Leicester, LE1 7RH, UK. hal18, ce14@le.ac.uk

The control law $\nu(t)$ is designed based on the pair (A, B_ν) which is assumed to be controllable. Once the design of $\nu(t)$ is complete, by direct manipulation, the true control signal $u(t)$ is recovered as $u(t) = N^\dagger \nu(t)$ where $N^\dagger \in \mathbb{R}^{m \times l}$ is a right pseudo-inverse of the matrix N . The choice of N^\dagger is not unique and different approaches have been proposed in the literature [22], [23], [29], [11], [3], [4], [16] for the choice of N^\dagger . The design procedure proposed in [1] will be considered here.

A. Design procedure

The design procedure can be summarized as follows:

1) Pre-design calculations:

- (i) Make a re-ordering of the states in (1) so that the input distribution matrix B is partitioned as:

$$B = \begin{bmatrix} B_1 \\ B_2 \end{bmatrix} \quad (3)$$

where $B_1 \in \mathbb{R}^{(n-l) \times m}$ and $B_2 \in \mathbb{R}^{l \times m}$ has rank l . In most aircraft systems, B_2 (which is intended to represent the dominant contribution of the control action on the system) is associated with the equations of angular acceleration in roll, pitch and yaw [16], while B_1 generally will have elements of small magnitude compared to B_2 .

- (ii) Scale the states of the system in (1) so that $B_2 B_2^T = I_l$ and therefore $\|B_2\| = 1$. This is always possible since $\text{rank}(B_2) = l$ by construction.
- (iii) Let the ‘virtual control’

$$\nu(t) := B_2 u(t) \quad (4)$$

so that

$$u(t) = B_2^\dagger \nu(t) \quad (5)$$

where the pseudo inverse is chosen as

$$B_2^\dagger := W B_2^T (B_2 W B_2^T)^{-1} \quad (6)$$

where $W \in \mathbb{R}^{m \times m}$ is a symmetric positive definite (s.p.d) diagonal weighting matrix. As suggested in [1], the weight W has been chosen as

$$W := I - K \quad (7)$$

and so $W = \text{diag}\{w_1, \dots, w_m\}$ where $w_i = 1 - k_i$. In a fault free situation $W = I$. As $k_i \rightarrow 1$, $w_i \rightarrow 0$ and so the associated component $u_i \rightarrow 0$.

- (iv) Define

$$\hat{\nu}(t) := (B_2 W^2 B_2^T) (B_2 W B_2^T)^{-1} \nu(t) \quad (8)$$

and change coordinates using the linear transformation $x(t) \mapsto \hat{x}(t) = T_r x(t)$ where

$$T_r := \begin{bmatrix} I & -B_1 B_2^T \\ 0 & I \end{bmatrix} \quad (9)$$

It can be shown in [1] that in the new coordinates

$$\begin{bmatrix} \dot{\hat{x}}_1 \\ \dot{\hat{x}}_2 \end{bmatrix} = \underbrace{\begin{bmatrix} \hat{A}_{11} & \hat{A}_{12} \\ \hat{A}_{21} & \hat{A}_{22} \end{bmatrix}}_{\hat{A}} \begin{bmatrix} \hat{x}_1 \\ \hat{x}_2 \end{bmatrix} + \underbrace{\begin{bmatrix} 0 \\ I \end{bmatrix}}_{\hat{B}} \hat{\nu} + \begin{bmatrix} B_1 B_2^N B_2^+ \\ 0 \end{bmatrix} \hat{\nu} \quad (10)$$

where

$$B_2^+ := W^2 B_2^T (B_2 W^2 B_2^T)^{-1} \quad (11)$$

and

$$B_2^N := (I - B_2^T B_2) \quad (12)$$

In (10) the state $\hat{x}_1 \in \mathbb{R}^{(n-l)}$ and $\hat{x}_2 \in \mathbb{R}^l$.

- (v) Compute the smallest possible scalar γ_0 so that

$$\|B_2^+\| = \|W^2 B_2^T (B_2 W^2 B_2^T)^{-1}\| < \gamma_0, \quad (13)$$

for all $0 < W \leq I$. It is argued in [1] that a finite value of γ_0 exists.

2) Design of matrix M :

- (i) The selection of the sliding surface is the first part of any sliding mode design and defines the system’s closed-loop performance. Define a switching function $\sigma(t) : \mathbb{R}^n \rightarrow \mathbb{R}^l$ to be

$$\sigma(t) = Sx(t)$$

where $S \in \mathbb{R}^{l \times n}$ and $\det(SB_\nu) \neq 0$. Let \mathcal{S} be the hyperplane defined by $\mathcal{S} = \{x(t) \in \mathbb{R}^n : Sx(t) = 0\}$. If a control law can be developed which forces the closed-loop trajectories onto the surface \mathcal{S} in finite time and constrains the states to remain there, then an ideal sliding motion has been attained [12]. In the $\hat{x}(t)$ coordinates in (10), a choice for the sliding surface is

$$\hat{\mathcal{S}} := ST_r^{-1} = [M \quad I_l] \quad (14)$$

where $M \in \mathbb{R}^{l \times (n-l)}$ represents design freedom. The design objective is to compute M from (14) so that $\hat{A}_{11} := \hat{A}_{11} - \hat{A}_{12}M$ is stable. If (\hat{A}, \hat{B}) is controllable, then $(\hat{A}_{11}, \hat{A}_{12})$ is controllable [12] and a matrix M can always be found to make \hat{A}_{11} stable.

3) Stability analysis:

- (i) Check that

$$\gamma_1 := \|MB_1 B_2^N\| < \frac{1}{\gamma_0} \quad (15)$$

is satisfied where γ_0 is given in (13). Otherwise re-design the matrix M .

- (ii) Define

$$\tilde{G}(s) := \tilde{A}_{21}(sI - \tilde{A}_{11})^{-1} B_1 B_2^N \quad (16)$$

where s represents the Laplace variable and the matrix $\tilde{A}_{21} := M\hat{A}_{11} + \hat{A}_{21} - \hat{A}_{22}M$. By construction the transfer function $\tilde{G}(s)$ is stable. Define

$$\|\tilde{G}(s)\|_\infty = \gamma_2 \quad (17)$$

- (iii) If $\gamma_2 < \frac{1}{\gamma_0} - \gamma_1$, then as shown in [1] the closed loop is guaranteed to be stable $\forall 0 < W \leq I$. Otherwise re-design the matrix M . Both γ_1 and γ_2 depend on the design of the sliding surface since they depend on M . However they are independent of W . The scalar γ_0 depends on W but is independent of M .

4) Obtaining the control law:

- (i) The final aspect of the control design, is the synthesis of a control law to guarantee that the surface is reached in finite time and a sliding mode is subsequently maintained. The proposed virtual control law from [1] has a structure given by $\hat{v}(t) = \hat{v}_l(t) + \hat{v}_n(t)$ where

$$\hat{v}_l(t) := -\tilde{A}_{21}\hat{x}_1(t) - \tilde{A}_{22}\sigma(t) \quad (18)$$

where $\tilde{A}_{22} := M\hat{A}_{12} + \hat{A}_{22}$ and the nonlinear component is defined to be

$$\hat{v}_n(t) := -\rho(t, x) \frac{\sigma(t)}{\|\sigma(t)\|} \quad \text{for } \sigma(t) \neq 0 \quad (19)$$

where $\sigma(t) = \hat{S}\hat{x}(t)$. The nonlinear gain

$$\rho(t, x) := \frac{\gamma_1\gamma_0\|\hat{v}_l(t)\| + \eta}{1 - \gamma_1\gamma_0} \quad (20)$$

ensures sliding takes place on \mathcal{S} in finite time [1].

- (ii) The final control law is

$$u(t) = WB_2^T(B_2W^2B_2^T)^{-1}\hat{v}(t) \quad (21)$$

III. FTLAB747

FTLAB747 has become one of the most well developed and established nonlinear aircraft models in the open literature. Running under MATLAB, the software has been used by various researchers – as part of an independent investigation of the ELAL flight 1862 incident [25] and for testing FTC and FDI schemes (see for example Marcos *et al.*[20], Maciejowski & Jones [18]). This high fidelity simulation model will be used to test the PCA ideas from the earlier section. The idea is to design a longitudinal and a lateral controller for nominal conditions, which can also be used when actuator faults or failures occur. Here, the loss of all the control surfaces, associated with a total hydraulic failure, will be considered. The main objective is to be able to change the heading of the aircraft and to descend to an altitude safe for landing. This can be achieved by tracking an appropriate roll angle (ϕ) command (while the β command is set to zero) using the lateral controller, and tracking a flight path angle (FPA) command using the longitudinal controller.

A linearization of the fault free aircraft has been obtained around an operating condition of 263,000 Kg, 92.6 m/s (180 Kn) true airspeed, 0 deg flaps and an altitude of 600m. This condition is quite similar to the flight condition used in [8] (page 21). In the following state-space representation, all the inputs have been individually scaled which results in two system and input distribution matrix pairs

$$A_{lat} = \begin{bmatrix} -0.7944 & 0.5355 & -1.1691 & 0.0009 \\ -0.0395 & -0.1182 & 0.2279 & -0.0016 \\ 0.2093 & -0.9723 & -0.0886 & 0.1039 \\ 1.0000 & 0.1984 & 0 & 0 \end{bmatrix} \quad (22)$$

$$B_{lat} = \begin{bmatrix} -0.0703 & 0.0703 & -0.2159 & 0.2159 & -0.1144 & -0.0206 \\ -0.0063 & 0.0063 & -0.0144 & 0.0144 & -0.0102 & -0.0023 \\ 0 & 0 & 0 & 0 & 0.0003 & 0.0001 \\ 0 & 0 & 0 & 0 & 0 & 0 \\ 0.0206 & 0.1144 & 0.0855 & 0.0220 & 0.0125 & -0.0125 \\ 0.0023 & 0.0102 & -0.2347 & 0.1133 & 0.0647 & -0.0647 \\ -0.0001 & -0.0003 & 0.0171 & 0 & 0.0005 & -0.0005 \\ 0 & 0 & 0 & 0 & 0 & 0 \end{bmatrix} \quad (23)$$

$$\left. \begin{array}{l} -0.0220 \\ -0.1133 \\ -0.0005 \\ 0 \end{array} \right\} \begin{array}{l} B_{lat,2} \\ B_{lat,1} \end{array}$$

and

$$A_{long} = \begin{bmatrix} -0.5137 & -0.0948 & 0 \\ 1.0064 & -0.2594 & 0 \\ 1.0000 & 0 & 0 \end{bmatrix} \quad (24)$$

$$B_{long} = \begin{bmatrix} -0.6228 & -1.3578 & 0.0540 \\ -0.0352 & -0.0819 & -0.0136 \\ 0 & 0 & 0 \end{bmatrix} \quad \left. \begin{array}{l} \\ \\ \end{array} \right\} \begin{array}{l} B_{long,2} \\ B_{long,1} \end{array} \quad (25)$$

where the states represent $x_{lat} = [p \ r \ \beta \ \phi]^T$ and $x_{long} = [q \ \alpha \ \theta]^T$. The lateral control surfaces are $\delta_{lat} = [\delta_{air} \ \delta_{ail} \ \delta_{aor} \ \delta_{aol} \ \delta_{sp1-4} \ \delta_{sp5} \ \delta_{sp8} \ \delta_{sp9-12} \ \delta_r \ e_1 \ e_2 \ e_3 \ e_4]^T$ which represent aileron deflection (right & left - inner & outer)(rad), spoiler deflections (left: 1-4 & 5 & right: 8 & 9-12) (rad), rudder deflection (rad) and lateral engine pressure ratios (EPR). The longitudinal control surfaces are $\delta_{long} = [\delta_e \ \delta_s \ e_c]^T$ which represent elevator deflection (rad), horizontal stabilizer deflection (rad), and collective EPR. The partitions of the input distribution matrices in (23) and (25) show the terms B_1 and B_2 (although a further change of coordinates is necessary to obtain the form in (3) and to scale B_2 to ensure $B_2B_2^T = I$). The dimensions of the virtual control in both cases are $l_{lat} = 2$ and $l_{long} = 1$. The controlled outputs are ϕ and β for lateral control, and FPA for longitudinal control. These linear models of the *nominal damage free aircraft* will be used to design the control schemes which will be described in the next sections. This is a major difference compared to [18] for example, where the MPC controller is designed based on exact knowledge of the post-damage aircraft.

A. B747 Fault Tolerant Controller Design

For tracking purposes, integral action has been included for both longitudinal and lateral control. Details can be found in [28], [12].

1) *Lateral Controller Design:* For lateral control, the sliding surface matrix M is chosen to minimize a quadratic performance index [28], [12]. A s.p.d matrix Q is used to tune the closed-loop response. Here, the weighting matrix has been chosen as $Q_{lat} = \text{diag}(0.005, 0.1, 50, 50, 1, 1)$. The first two terms of Q_{lat} are associated with the integral action and are less heavily weighted. The 3rd and 4th terms of Q_{lat} are associated with the equations of angular acceleration in roll (i.e. the $B_{lat,2}$ term partition in (3)) and weight the ‘virtual control term’. By analogy to a more typical LQR framework, it affects the speed of response of the closed-loop system. Here, the second term of Q_{lat} has been heavily weighted compared to the last four terms. The poles associated with the reduced order sliding

motion are $\{-0.0715, -0.1333, -0.1724 \pm 0.1354i\}$. In the simulations, the discontinuity in the nonlinear control term in (19) has been smoothed by using a sigmoidal approximation $\frac{\sigma_{lat}}{\|\sigma_{lat}\| + \delta_{lat}}$, where the scalar $\delta_{lat} = 0.05$ (see for example §3.7 in [12]). This removes the discontinuity and introduces a further degree of tuning to accommodate the actuator rate limits – especially during actuator fault or failure conditions. In normal operation, the ailerons and spoilers will be the primary control surfaces for ϕ tracking, whilst the differential thrust from the four engines is the associated redundancy. Based on these assumptions, it can be verified from a numerical search that $\gamma_{0_{lat}}$ from (13) is $\gamma_{0_{lat}} = 4.6163$. Simple calculations from (15) show that $\gamma_{1_{lat}} = 0.0050$, and therefore $\gamma_{0_{lat}}\gamma_{1_{lat}} = 0.0232 < 1$. For this particular choice of sliding surface, $\|\tilde{G}_{lat}(s)\|_\infty = \gamma_{2_{lat}} = 0.1489$ from (17). Therefore

$$\frac{\gamma_{2_{lat}}\gamma_{0_{lat}}}{1 - \gamma_{1_{lat}}\gamma_{0_{lat}}} = 0.7034 < 1$$

which shows that the system is stable for all $0 < w_i \leq 1$. To introduce real aircraft flight control capability, an outer loop PID heading control, similar to the one in [2], is used to provide a roll command to the inner-loop sliding mode controller. The proportional gain has been chosen as $K_{p_{lat}} = 3$, the integrator gain as $K_{i_{lat}} = 0.1$ and the derivative gain as $K_{d_{lat}} = 3$. Note that the integrator component is only activated when the heading angle error is less than 5° to eliminate steady state error.

2) *Longitudinal Controller Design:* As in the lateral controller design, a quadratic optimal design has been used to obtain the sliding surface matrix. The s.p.d weighting matrix has been chosen as $Q_{long} = \text{diag}(0.1, 2, 1, 1)$. Again, similar to the lateral controller design, the first term of Q_{long} is associated with the integral action and is less heavily weighted. The second term of Q_{long} is associated with the $B_{long,2}$ term partition in (3) (i.e. pitch acceleration) and weights the virtual control term. This has been heavily weighted compared to the last two terms. The poles associated with the reduced order sliding motion are $\{-1.0351, -0.1859 \pm 0.1422i, \}$. As in the lateral controller, the discontinuity in the nonlinear control term in (19) has been smoothed by using a sigmoidal approximation where the scalar $\delta_{long} = 0.05$. In normal operation, the elevators will be the primary control surface for FPA tracking, whilst the horizontal stabilizer and collective thrust introduce redundancy. It will be assumed that at least the collective thrust for FPA tracking will be available when a fault or failure occurs. Based on these assumptions, it can be verified from a numerical search that $\gamma_{0_{long}} = 27.7063$. Simple calculations from (15) show that $\gamma_{1_{long}} = 0.0066$, therefore $\gamma_{0_{long}}\gamma_{1_{long}} = 0.1838 < 1$. For this choice of sliding surface $\|\tilde{G}_{long}(s)\|_\infty = \gamma_{2_{long}} = 0.0024$ and therefore

$$\frac{\gamma_{2_{long}}\gamma_{0_{long}}}{1 - \gamma_{1_{long}}\gamma_{0_{long}}} = 0.0816 < 1$$

which shows that the system is stable for all choices of $0 < w_i \leq 1$. Again, to emulate real aircraft flight control

capability, an outer loop PID altitude controller, is used to provide a FPA command to the inner loop sliding mode controller. The proportional gain was set as $K_{p_{long}} = 0.001$, the integrator gain was set as $K_{i_{long}} = 0.00004$ and the derivative gain $K_{d_{long}} = 0.02$. The integrator component is only activated when the altitude error is less than 15m.

In addition, a PID is used to regulate V_{tas} . The proportional and derivative gains are $K_p = 0.2, K_d = 0.05$ respectively. In the event of total hydraulic failure, speed control will no longer be of prime concern because of the conflicting requirement of FPA control. During a failure, the thrust must be employed to manipulate FPA. In the simulations, ‘control mixing’ was employed, where the signals from both the lateral controller (e_1, e_2, e_3 and e_4) and longitudinal controller (e_c) were added together before being applied to each of the engines (page 14 of [9]).

B. B747 Fault Tolerant Control Simulation Results

The simulations presented in this paper are all based on FTLAB747 which represents the *full 77 state non-linear model*. In this paper, the information necessary to compute W will be supplied by assuming measurements of the actual actuator deflections are available. This is common in passenger aircraft [5].

To illustrate the results, a landing approach manoeuvre with a low speed configuration, has been considered as shown in Figure 1. Compared to the flight conditions in [8] (page 21), a much lower speed of 92.6m/s is chosen. Note that a speed of 92.6m/s V_{tas} is slow with a 0° flap setting. This is outside the aircraft’s ‘comfort’ zone, as normally at this speed, the aircraft requires the flaps to be extended (or in the case of 0° flaps, a higher landing speed is required [14]). This adds more challenges and further tests the capability of the controller. As a comparison, the same manoeuvres are tested on both the fault-free and total hydraulic failure case. The objective is to fly the aircraft to a near landing condition on a runway. The aircraft heads towards the centreline of the runway at an angle of 90° (Figure 1). Shortly after (at 50s), the aircraft is required to change heading to 0° to line up with the runway. At 250s, the aircraft will also be required to descend to an altitude of 50m above the runway and bring the aircraft to the landing target zone. The flare and the actual landing of the aircraft are not carried out and the simulation was stopped shortly after the altitude 50m is achieved (500s). Figure 1 shows that there is a small difference between the fault-free trajectory and the total hydraulic failure case after the heading change. This is due to the change in speed for the failure case (speed control is sacrificed for FPA tracking and no ILS guidance is available). This indicates that the controller is able to provide good performance when using engines as the only means to control the aircraft for the failure case.

Figures 2-3 show the states and the control surface deflections for the fault-free condition. The aircraft has an initial -90° heading hold prior to heading change, and the outer loop PID heading control provides an inner loop roll angle demand to guide the aircraft towards a heading

of 0° (Figure 2). Note that in the original B747-100/200 controller, the roll demand is limited to 15° during the final approach stages [14] which is considered here. After 250s, the altitude change is activated and the outer loop altitude control provides a FPA demand to guide the aircraft to a new altitude of 50m above the runway. The sideslip and V_{tas} commands are fixed at 0° and 92.6m/s respectively. The fault-free variation in the lateral and longitudinal switching function signals are shown in Figure 4.

Figures 5-6 show the states and the control surface deflections for the total hydraulic failure case. Figure 5 shows similar tracking performance compared to the nominal case except for V_{tas} . This is due to the fact that there is no V_{tas} outer loop PID control, to give priority to FPA control due to lack of redundancy, since the engines are the only actuators left to be manipulated. The speed fluctuation however is still within the range of the results obtained by NASA in [9], [8]. Figure 6, shows that after total hydraulic failure, all control surfaces become inactive except for the EPRs. Small oscillations are visible during the start of the roll and FPA manoeuvres to damp the aircraft oscillatory mode but they quickly disappear. The characteristics and the range of the EPR signals are comparable to the results obtained by NASA in [9], [8]. The switching function signals in Figure 7, shows small deviations compared to the one in Figure 4. This represents the extra effort needed to maintain the nominal performance after the failure has occurred and highlight the level of difficulty of the failure.

IV. CONCLUSIONS

This paper has demonstrated the possibility of controlling an aircraft using only engine thrust (in the event of total loss of hydraulics) based on a recently developed on-line sliding mode control allocation scheme. The simulations have been undertaken on the MATLAB based model FT-LAB747, which represents one of the most detailed aircraft models in the open literature. The effectiveness level of the actuators is used by the control allocation scheme to redistribute the control signals to modulate engine thrust when a total hydraulic failure occurs. The implemented results have shown that not only can the controller perform well in nominal flight conditions, but is also able to maintain performance under total hydraulic failure by re-distributing the control signals.

REFERENCES

- [1] H. Alwi and C. Edwards. Fault tolerant control using sliding modes with on-line control allocation. *Automatica*, 44(7):1859–1866, 2008.
- [2] H. Alwi, C. Edwards, O. Stroosma, and J. A. Mulder. Piloted sliding mode FTC simulator evaluation for the ELAL Flight 1862 incident. In *AIAA Guidance, Navigation, and Control Conference*, 2008.
- [3] K. A. Bordignon and W. C. Durham. Closed-form solutions to constrained control allocation problem. *AIAA Journal of Guidance, Control, and Dynamics*, 18(5):1000–1007, 1995.
- [4] J. D. Bošković and R. K. Mehra. Control allocation in overactuated aircraft under position and rate limiting. In *Proceedings of the American Control Conference*, pages 791–796, 2002.
- [5] D. Brière and P. Traverse. Airbus A320/A330/A340 electrical flight controls: A family of fault-tolerant systems. *Digest of Papers FTCS-23 The Twenty-Third International Symposium on Fault-Tolerant Computing*, pages 616–623, 1993.
- [6] F. W. Burcham, J. Burken, T. A. Maine, and J. Bull. Emergency flight control using only engine thrust and lateral center-of-gravity offset: A first look. Technical Memorandum NASA/TM-4789, NASA, 1997.
- [7] F. W. Burcham, C. G. Fullertron, and T. A. Maine. Manual manipulation of engine throttles for emergency flight control. Technical Report NASA/TM-2004-212045, NASA, 2004.
- [8] F. W. Burcham, T. A. Maine, J. Burken, and J. Bull. Using engine thrust for emergency flight control: MD-11 and B-747 results. Technical Memorandum NASA/TM-1998-206552, NASA, 1998.
- [9] F. W. Burcham, T. A. Maine, J. Kaneshinge, and J. Bull. Simulator evaluation of simplified propulsion-only emergency flight control system on transport aircraft. Technical Report NASA/TM-1999-206578, NASA, 1999.
- [10] J. Cieslak, D. Henry, A. Zolghadri, and P. Goupil. Development of an active fault-tolerant flight control strategy. *AIAA Journal of Guidance, Control and Dynamics*, 31(1):135–147, 2008.
- [11] J. B. Davidson, F. J. Lallman, and W. T. Bundick. Real-time adaptive control allocation applied to a high performance aircraft. In *5th SIAM Conference on Control & Its Application*, 2001.
- [12] C. Edwards and S. K. Spurgeon. *Sliding Mode Control: Theory and Applications*. Taylor & Francis, 1998.
- [13] R. Hallouzi and M. Verhaegen. Fault-tolerant subspace predictive control applied to a Boeing 747 model. *AIAA Journal of Guidance, Control and Dynamics*, 31(4):873–883, 2008.
- [14] C. Hanke and D. Nordwall. The simulation of a jumbo jet transport aircraft. Volume II: Modelling data. Technical Report CR-114494/D6-30643-VOL2, NASA and The Boeing Company, 1970.
- [15] M. Harefors and D. G. Bates. Integrated propulsion-based flight control system design for a civil transport aircraft. *International Journal of Turbo and Jet Engines*, 20:95–114, 2003.
- [16] O. Härkegård and S. T. Glad. Resolving actuator redundancy - optimal control vs. control allocation. *Automatica*, 41(1):137–144, 2005.
- [17] T. J. J. Lombaerts, Q. P. Chu, J. A. Mulder, and D. A. Joosten. Real time damaged aircraft model identification for reconfiguring flight control. In *AIAA Atmospheric Flight Mechanics Conference and Exhibit*, 2007.
- [18] J. M. Maciejowski and C. N. Jones. MPC fault-tolerant control case study: flight 1862. In *Proceedings of the IFAC Symposium SAFEPROCESS '03, Washington*, 2003.
- [19] A. Marcos and G. J. Balas. A Boeing 747-100/200 aircraft fault tolerant and diagnostic benchmark. Technical Report AEM-UoM-2003-1, Department of Aerospace and Engineering Mechanics, University of Minnesota, 2003.
- [20] A. Marcos, S. Ganguli, and G. J. Balas. An application of H_∞ fault detection and isolation to a transport aircraft. *Control Engineering Practice*, 13:105–119, 2005.
- [21] Y. Ochi. Flight control system design for propulsion-controlled aircraft. *Proc. Institution of Mechanical Engineers, Part G: J. Aerospace Engineering*, 219:329–340, 2005.
- [22] D. Shin, G. Moon, and Y. Kim. Design of reconfigurable flight control system using adaptive sliding mode control: actuator fault. *Proceedings of the Institution of Mechanical Engineers, Part G (Journal of Aerospace Engineering)*, 219:321–328, 2005.
- [23] Y. Shtessel, J. Buffington, and S. Banda. Tailless aircraft flight control using multiple time scale re-configurable sliding modes. *IEEE Transactions on Control Systems Technology*, 10:288–296, 2002.
- [24] M. H. Smaili, J. Breeman, T. J. J. Lombaerts, and D. A. Joosten. A simulation benchmark for integrated fault tolerant flight control evaluation. In *AIAA Modeling and Simulation Technologies Conference and Exhibit*, 2006.
- [25] M. H. Smaili and J. A. Mulder. Flight data reconstruction and simulation of the 1992 Amsterdam Bijlmermeer airplane accident. In *AIAA Modeling and Simulation Technologies Conference*, 2000.
- [26] O. Stroosma, H. Smaili, T. Lombaerts, and J. A. Mulder. Piloted simulator evaluation of new fault-tolerant flight control algorithms for reconstructed accident scenarios. In *AIAA Modeling and Simulation Technologies Conference and Exhibit*, 2008.
- [27] C. P. Tan and C. Edwards. Sliding mode observers for robust detection and reconstruction of actuator and sensor faults. *International Journal of Robust and Nonlinear Control*, 13:443–463, 2003.
- [28] V. I. Utkin. *Sliding Modes in Control Optimization*. Springer-Verlag, Berlin, 1992.
- [29] S. R. Wells and R. A. Hess. Multi-input/multi-output sliding mode control for a tailless fighter aircraft. *Journal of Guidance, Control and Dynamics*, 26:463–473, 2003.

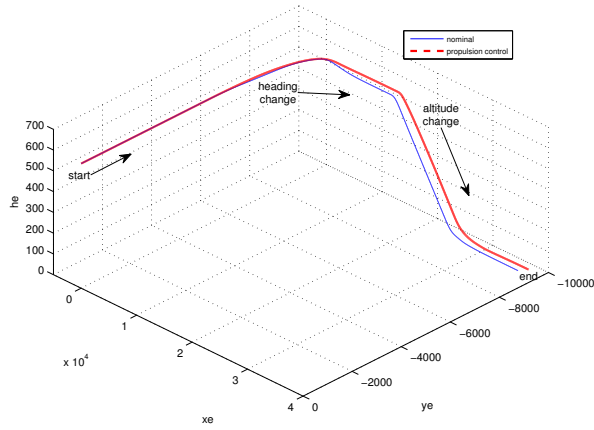


Fig. 1. 3-D flight trajectory

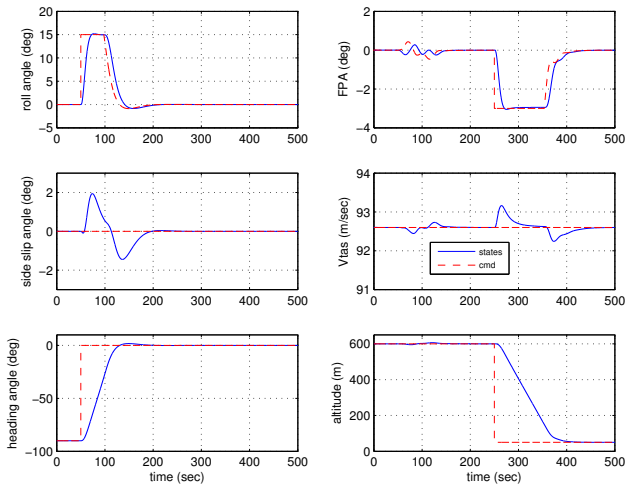


Fig. 2. nominal condition: controlled states

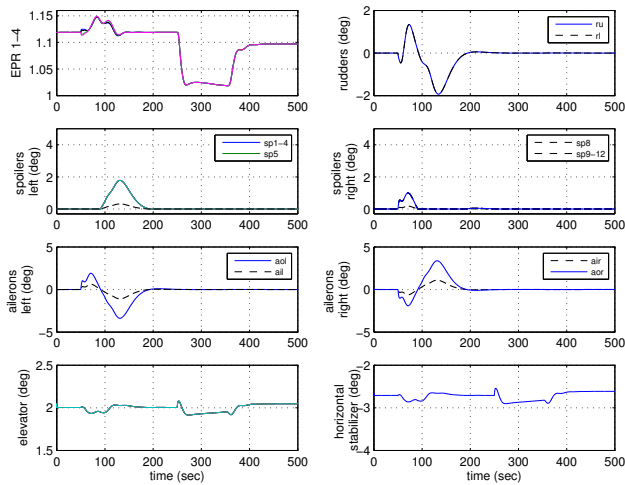


Fig. 3. nominal condition: control surface deflections

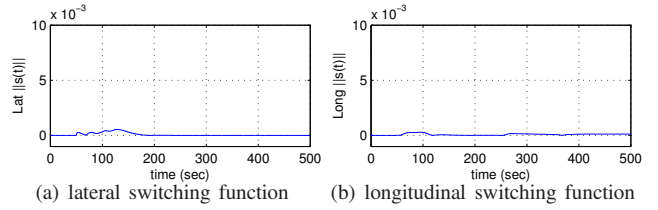


Fig. 4. nominal condition: switching function

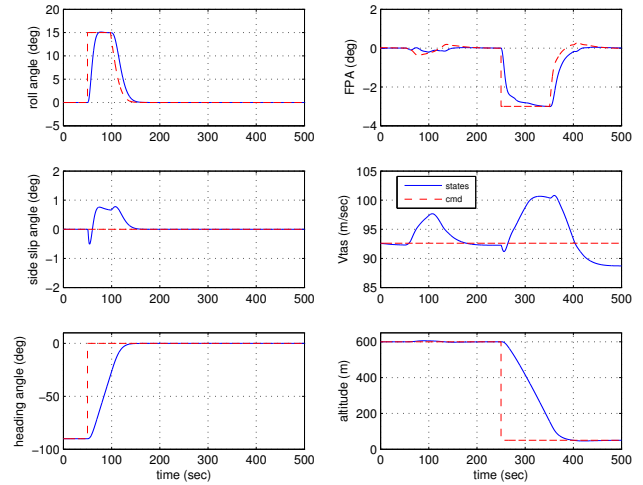


Fig. 5. propulsion control: controlled states

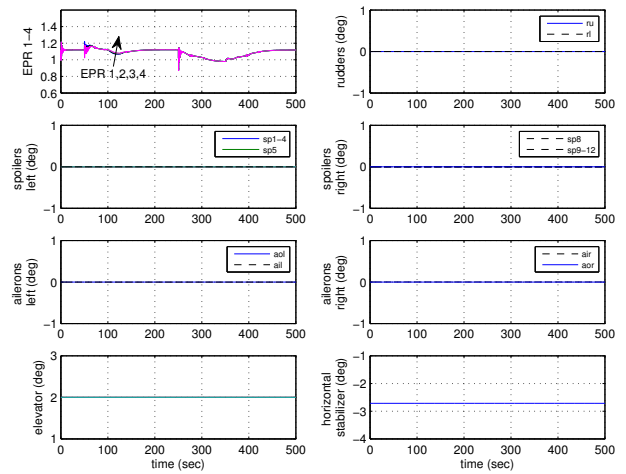


Fig. 6. propulsion control: control surface deflections

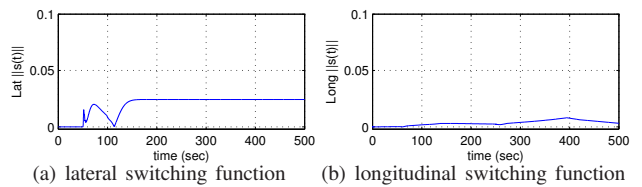


Fig. 7. propulsion control: switching function